STATISTICS IN MEDICINE
Statist. Med. 2003; **22**:2943–2961 (DOI: 10.1002/sim.1535)

Measuring spatial effects in time to event data: a case study using months from angiography to coronary artery bypass graft (CABG)

Angela M. Crook[1,2,*,†], Leonhard Knorr-Held[3] and Harry Hemingway[2,4]

[1]*Department of Epidemiology and Public Health, Imperial College, London, U.K.*
[2]*Department of Public Health Research, Westminster PCT, London, U.K.*
[3]*Medical Statistics Unit, Department of Mathematics and Statistics, Lancaster University, U.K.*
[4]*Department of Epidemiology and Public Health, UCL, London, U.K.*

SUMMARY

The application of Bayesian hierarchical models to measure spatial effects in time to event data has not been widely reported. This case study aims to estimate the effect of area of residence on waiting times to coronary artery bypass graft (CABG) and to assess the role of important individual specific covariates (age, sex and disease severity). The data involved all patients with definite coronary artery disease who were referred to one cardiothoracic unit from five contiguous health authorities covering 488 electoral wards (areas). Time to event was the waiting time in months from angiography (diagnosis) to CABG (event). A number of discrete time survival models were fitted to the data. A discrete baseline hazard was estimated by fitting waiting time non-parametrically into the models. Ward was fitted as a spatial effect using a Gaussian Markov random field prior. Individual specific covariates considered were age, sex and number of diseased vessels. The recently proposed DIC criteria was used for comparing models. Results showed a marked spatial effect on time to bypass surgery after including age, sex and disease severity in the model. Notably this spatial effect was not apparent when these covariates were not included in the model. The observed small area spatial variation in time to CABG warrants further investigation. Copyright © 2003 John Wiley & Sons, Ltd.

KEY WORDS: spatial; small area; time to event; Bayesian hierarchical models; CABG

INTRODUCTION

Describing and explaining small area variations in health outcomes is important for identifying potential inequalities in health care. Many studies investigate area variations taking no account of location using unstructured random effects models [1, 2]. Fewer studies have used spatial methods in which areas sharing a common boundary (neighbours) are assumed to be more similar to each other than to non-neighbours. Classical statistical methods encounter difficulties

*Correspondence to: Angela M. Crook, Department of Epidemiology and Public Health, Imperial College Faculty of Medicine, Norfolk Place, London, W2 1PG, U.K.
†E-mail: Angela.Crook@imperial.ac.uk

Received December 2001
Accepted December 2002

with estimating small area spatial effects when adjusting for other covariates. Recent advances in computing have led to an increase in the use of Markov chain Monte Carlo (MCMC) methods to build Bayesian hierarchical models to estimate area effects in a disease mapping context [3–5]. These models incorporate structured (spatial) random effects to capture the unmeasured area-level covariates, as it is rarely possible to measure all possible explanatory variables. Since the number of events in small areas may be sparse, smoothing techniques are required to increase precision of these effects. In a Bayesian context this involves the use of smoothing priors [6, 4]. The hierarchy of the model develops further with the specification of hyperpriors on the unknown variance parameter of the random effects.

Health outcomes commonly involve a time to event response such as waiting time for an operation. However, using a standard Cox proportional hazards model to estimate small area effects can be problematic if the number of unique failure times and unique covariate categories become large. In a spatial analysis with a large number of small areas and even a small number of covariates, this is a particular problem. One potential solution, investigated here, is to restructure the data and consider it as binary longitudinal by combining risk sets containing failed and censored events within each time interval [7–10]. A constant hazard is assumed over short time intervals. Bayesian smoothing priors can be used to provide semi-parametric estimates of the baseline hazard parameters and other quantitative covariate effects in the model [4].

We present here a case study of the spatial analysis of the time to event data involving patient waiting times from coronary angiography to surgical revascularization, coronary artery bypass graft (CABG). There are gross geographical differences in revascularization rates, for example, age standardized revascularization rates per 100 000 residents vary from 4 (Nottingham health authority) to 140 (Brent and Harrow health authority) [11]. However, these figures take no account of the rate of investigation (angiography) or the severity of angiographically defined disease. The issue of waiting times has attracted the attention of clinicians and policy makers internationally [12, 13]. It is reasonable to assume that the underlying risks, or hazards, of CABG in neighbouring areas are spatially correlated when potential (relevant but unobserved) spatial covariates include social factors such as area deprivation [14] and the referral process between physicians, cardiologists and cardiothoracic surgeons. Previous studies often rely on proxy measures of need such as area CHD mortality or hospital admission rates [15, 16], which can lead to problems of ecological bias. We used data from the Appropriateness of Coronary Revascularization (ACRE) study [17], which offers two strengths. First, the study population provides a clearly defined denominator, patients who undergo angiography, a prerequisite for undergoing surgery (numerator). Second, covariates are measured at the individual level and in particular the angiogram result provides 'precise' measurement of the single most important predictor of CABG, severity of coronary disease.

The aim of this study was to measure the spatial effect of area of residence on waiting time to an initial revascularization of CABG, in order to identify geographical areas of increased and decreased risk using Bayesian hierarchical modelling. We wanted to compare the area effects across two resolutions: health authority and electoral ward. Secondly, we wanted to assess the spatial effect with and without important individual level covariates by using the recently proposed deviance information criteria (DIC) [18]. We were interested in determining the amount of spatial variability in time to CABG among a diseased population who were all potential CABG candidates. Therefore we restricted this analysis to individual covariates with all unmeasured or unknown area specific factors considered as the (residual) spatial effect.

DATA

Patients and areas

We analysed data from 3015 patients with coronary artery disease defined at angiography. These patients were consecutive admissions during one year, from 15 April 1996, to Barts and the London NHS Trust as part of the ACRE study. Referrals for angiography came from five contiguous health authorities in the City and East London and Essex covering 488 electoral wards and a resident population of 2.8 million. All patients had coronary disease (including minimal disease) and so were considered to be at risk of CABG. Patients were followed up for a median of 2.5 years and by 14 April 1999, 995 (33 per cent) patients had undergone CABG.

Electoral ward and health authority (HA) boundaries defined the areas for the analysis (based on unit postcode of the patient's residence, 1991). Individual level covariates considered were age at time of angiography, sex and severity of coronary disease. Severity was measured at angiography by the number of diseased vessels: $1, 2, 3$.

Table I shows the breakdown of area and patient characteristics by health authority. Wards where no angiography procedures occurred during the study period were in East London and City and North Essex health authorities. More angiography procedures occurred in Redbridge and Waltham Forrest compared to the number of CABG procedures in that area. Median age for patients with coronary disease was 62 years; 23 per cent of these patients were female and 29 per cent had three-vessel (severe) disease. There were no marked differences in the age and sex distribution across health authorities. The pattern of coronary disease was also similar at health authority level.

Time to event (failure) was measured (in days) from date of angiography to date of an initial revascularization of CABG. Patients undergoing coronary angioplasty (PTCA) were censored at their procedure date as they were no longer considered to be at risk of an initial

Table I. Area and patient characteristics. Values are median (range) unless otherwise stated.

Health Authority	East London and City	Barking and Havering	Redbridge and Waltham Forrest	South Essex	North Essex	Total
Areas						
Wards (n)	91	44	41	96	216	488
Wards with patients (n)	69	44	41	94	178	426
Angiograms per ward	9 (0–31)	11 (6–21)	19 (8–42)	8 (0–25)	2 (0–16)	6 (0–42)
Patients with CAD per ward	7 (0–26)	10 (3–17)	15 (7–32)	7 (0–21)	2 (0–13)	5 (0–32)
CABG procedures per ward	2 (0–10)	4 (2–10)	3 (0–12)	2 (0–9)	1 (0–7)	2 (0–12)
Patients with CAD (n)	653	437	651	703	571	3015
Waiting time (median days)	148	246	242	175	171	209
Age (median years)	61	63	61	62	62	62
Female (per cent)	25	26	23	22	22	23
Number of diseased vessels						
1 DV (per cent)	43	48	48	47	43	46
2 DV (per cent)	28	23	23	25	28	25
3 DV (per cent)	29	29	29	28	29	29

revascularization of CABG. Patients who died without undergoing any procedure were censored at their date of death. The remaining medically managed patients were censored at 14 April 1999. Median CABG waiting times ranged from 148 days to 246 days between health authorities.

The data were restructured by splitting the waiting times (both failed and censored) into $t = 36$ monthly time intervals. Risk sets for each interval were then combined, increasing the number of 'observations' to 49 598. The dependent variable was then now binary: a person either underwent CABG or did not, during month t, conditional on no surgery up to month t. A discrete baseline hazard was estimated non-parametrically and assumed to be constant during each monthly interval t, with non-informative censoring occurring at the end of each month. A finer subdivision into weekly intervals would have resulted in a further increase to more than 200 000 observations, which would have caused computational problems and made screening of a series of models more difficult.

METHOD

Bayesian semi-parametric binary regression models [4] with a probit link function were fitted to this restructured data set. All models were estimated using BayesX [19], a software package that can analyse such regression models using MCMC simulation techniques. BayesX can handle complex data types, such as estimation of spatial effects and non-parametric estimation of continuous effects. This non-parametric smoothing capability within BayesX is an advantage over other MCMC software packages such as WinBUGS [20].

Let T denote the waiting time to CABG. The discrete hazard function (conditional probability of surgery during month t, given no surgery to beginning of month t) was modelled as

$$P(T = t \mid T \geqslant t) = \Phi(f_0(t) + f_1(\text{age}) + f_2(\text{ward}) + x'\beta)$$

where Φ is the cumulative distribution function of a standardized normal variable, the fs are appropriate smoothing functions of covariates such as age and ward and β represents the vector of fixed effects of covariates x (sex and number of diseased vessels). Specifying these smoothing priors was required to filter out random variation and so increase the reliability of the estimates.

To ensure identifiability, BayesX automatically imposes sum-to-zero constraints on the parameters representing the smooth functions f_0, f_1 and f_2 and includes an additional intercept term. This is implemented during the MCMC by subtracting the mean from the current estimate at each iteration. For convenience, we added this intercept to the baseline effect f_0.

Baseline and age were fitted non-parametrically with second-order random walk smoothing priors [21]. This model borrows strength from neighbouring parameters. For example, for the baseline effect h_0, second differences between neighbouring effects, $(h_{0t+1} - h_{0t}) - (h_{0t} - h_{0t-1}) = h_{0t+1} - 2h_{0t} + h_{0t-1}$, have variance σ^2_{rw} and

$$p(h_0 \mid \sigma^2_{\text{rw}}) \propto \exp\left(-\frac{1}{2\sigma^2_{\text{rw}}} \sum_{j=2}^{k-1} (h_{0t+1} - 2h_{0t} + h_{0t-1})^2\right)$$

The effect is to smooth estimates towards a linear trend of neighbouring parameters.

Ward was fitted as a spatially structured effect with a Markov random field smoothing prior [3]. This assumed areas to be more similar to their neighbours than to other arbitrary areas. Areas were defined as neighbours if they shared a common boundary. The area effect estimates, a_k, were smoothed towards a (local) mean effect estimate, m_k, of their neighbours, a_j

$$a_k \mid a_{j,j\neq k} \sim \mathrm{N}(m_k, \sigma_u^2/n_k)$$

where n_k is the number of neighbours.

We also fitted ward as an unstructured random effect (*a priori* independent). In this case the area effect estimates were smoothed towards the mean of the whole (combined) area

$$a_k \sim \mathrm{N}(0, \sigma_v^2)$$

We also considered formulations with both terms in order to let the data decide how much variation was spatially structured and how much was unstructured [3].

Health authority area was also fitted as a random effect as a more efficient alternative to fitting four dummy variables compared to an arbitrarily chosen reference health authority. Since there were only five health authorities in our study area, there was no need to borrow strength from neighbouring health authorities (in contrast to wards which were on a much finer spatial resolution) so we did not assume a spatial structure for the corresponding random effects.

Number of diseased vessels (2 diseased vessels (DV) and 3 DV versus 1 DV) and sex (female versus male) were fitted as fixed effects with diffuse priors. Finally, to test the proportional hazards assumption, time varying covariate effects were included in the model [8, 4].

The hierarchy of the Bayesian model is completed by specifying hyperpriors on the variances of the smoothing priors. The BayesX default is set with inverse gamma priors, IG(a, b), with $a = 1$ and $b = 0.005$, which were used for all effects except baseline and age which used $b = 0.00005$. Sensitivity to this choice was tested. Decreasing the value of b corresponds to a lower prior guess of the size of the variance, as the inverse gamma distribution has its mode at $b/(a + 1)$.

Details of results are presented from the following models:

Model 0: Baseline
Model 1: Baseline+Health Authority(random)
Model 2: Baseline+Ward(spatial)
Model 3: Baseline+Health Authority(random)+Ward(spatial)
Model 4: Baseline+Ward(random)
Model 5: Baseline+Ward(random)+Ward(spatial)
Model 6: Baseline+Age+Female+2DV+3DV
Model 7: Baseline+Age+Female+2DV+3DV+Health Authority(random)
Model 8: Baseline+Age+Female+2DV+3DV+Ward(spatial)
Model 9: Baseline+Age+Female+2DV+3DV+Ward(spatial)+Health Authority(random)
Model 10: Baseline+Age+Female+2DV+3DV+Ward(random)
Model 11: Baseline+Age+Female+2DV+3DV+Ward(random)+Ward(spatial)
Model 12: Baseline+ 2DV*Baseline+3DV*Baseline+Age+Female+Ward(spatial)

Model 0 is the null model with only the baseline effect fitted. In order to investigate what extra information could be gained from analysing (spatial) area effects using the ward level resolution, compared to using the larger health authority boundaries, models were fitted that included both these area effects separately (models 1 and 2) and together (model 3). The (strong) spatial prior imposed on the ward effects attempts to capture all unobserved spatial heterogeneity such as, for example, local hospital and GP effects. This spatial prior on the ward effects was compared to using an exchangeable prior, again separately (models 2 and 4) and together (model 5). All of these models were then fitted with the inclusion of individual covariates, of age, sex and number of diseased vessels (models 6 to 11). These models were then compared to their respective models without individual covariates. Finally, to test the proportional hazards assumption, selected time dependant covariates were included in models and details given for one (model 12).

The MCMC specification for each model was 11 000 iterations, the first 1000 discarded and every tenth subsequent sample point ($n = 1000$) saved for estimation of posterior medians and quantiles. Convergence to the stationary distribution was checked using S-plus functions provided on the BayesX homepage. These functions allow the routine plotting of autocorrelations of the samples from all parameters calculated within BayesX. BayesX code used for running selected models is included in an Appendix.

Marginal standard deviations, approximate hazard ratios and 95 per cent credible intervals and posterior probabilities of effect sizes were calculated. The model fit and complexity were compared by examining the distribution of the posterior deviance and by calculating the recently proposed deviance information criteria (DIC) [18]. This criterion penalizes the mean posterior deviance $\bar{D}$ (a measure of model fit) with a term p_D measuring model complexity, the so-called 'effective number of parameters', that is, $\mathrm{DIC} = \bar{D} + p_D$.

Choice of link function

The complementary log-log link function, as the discrete analogue of the proportional hazard model [22, 10], would be the natural choice for modelling this type of interval censored data. However it has been shown that a logit link can produce very similar results especially for small time intervals where the conditional probabilities for failure, $P(T = t \mid T \geqslant t)$, become small [22]. Here we chose a probit link function for computational reasons as a convenient approach to screen a number of different models.

There are considerable computational advantages using the probit formulation and an implementation based on latent variables. In particular, it allows for fast block updates of the parameters representing the non-parametric smoothing functions f_0, f_1 and f_2 [23, 24]. Furthermore, results using the probit model are qualitatively very similar to logit estimates [10]. Using the probit link as an approximation to the logit model is very common in many other areas of statistics, for example, in measurement error models as discussed in Carroll *et al.*, (reference [25], page 64f).

The disadvantage of using this link function is that the estimates are not directly interpretable like logit estimates that transform to give odds ratios. However, the difference between the logit and the probit link function is mainly a change of scale, so we approximated the probit estimates to logit estimates by multiplying by a factor $C = (\pi/\sqrt{3})^*(15/16)$ [25]. For simplicity, assume there is only one binary covariate x coded as 1 and 0. The exponent of the transformed estimate can be considered (to a good degree of accuracy) as the conditional

odds ratio

$$\frac{P(T=t \mid T \geqslant t, x=1)/P(T>t \mid T \geqslant t, x=1)}{P(T=t \mid T \geqslant t, x=0)/P(T>t \mid T \geqslant t, x=0)} = \frac{P(T=t \mid x=1)/P(T>t \mid x=1)}{P(T=t \mid x=0)/P(T>t \mid x=0)}$$

which is a close approximation to the hazard ratio

$$\frac{P(T=t \mid x=1)/P(T \geqslant t \mid x=1)}{P(T=t \mid x=0)/P(T \geqslant t \mid x=0)} = \frac{P(T=t \mid T \geqslant t, x=1)}{P(T=t \mid T \geqslant t, x=0)}$$

These approximations were used to ease interpretation of parameter estimates. Recently Holmes and Knorr-Held have shown how to implement the logistic regression model using a latent variable approach, which would avoid the need for these approximations [26]. However, this is not yet implemented in the BayesX software.

RESULTS

Table II gives the median posterior marginal standard deviations (SD) for all the models and details of model fit and complexity measured by $\bar{D}$, p_D and DIC. Table III gives (approximate) hazard ratio (HR) estimates for respective covariates in all the models.

Models without covariates (models 0–5)

The baseline effect of time to CABG (Figure 1) was similar for all models without covariates. This showed an initially high risk of CABG immediately post angiography. Between 6–16 months there was increasing risk. Sixteen months from angiography the chance of having surgery decreased.

Including a health authority effect on time to CABG (model 1) produced a small marginal SD estimate (95 per cent credible interval) of 0.04 (0.02,0.06). The HR (95 per cent credible interval) indicated a decreased risk in Redbridge and Waltham Forrest health authority, 0.92 (0.86,0.99) compared to the overall average. The DIC for this model of 9014.

The marginal SD for the spatial effect for model 2 without covariates was small, 0.07 with 95 per cent credible interval of 0.04–0.12. The range of ward HR estimates were from 0.84 to 1.15. Figure 2 displays the spatial estimates with dark areas indicating an increased effect on hazard of CABG while lighter areas show a decreased effect. For this model there was little evidence of any spatial variation. The second map in Figure 2 shows the posterior probabilities of these estimated effects. The black areas indicate that at least 95 per cent of sample hazard ratio estimates were completely greater than 1 (none for this model). White areas indicate that 0–5 per cent were greater than 1 and the grey areas are the remainder which were considered as 'non-significant'. The DIC for this model was 9003.

Fitting ward as an unstructured random effect (model 4) gave no improvement in terms of DIC. Including both health authority effects and spatial ward effect also made no improvement (model 3), similarly for fitting ward as a spatial and random effect (model 5).

Models with covariates (models 6–9)

Including age, sex and disease severity reduces the DIC to 8533 (from 9020). The model fit improved significantly to 8514 while p_D increased to 19. The effect of age (Figure 3) was

Table II. Results from models 0–12. Values are posterior median estimates of *Marginal standard deviation* with 95 per cent credible intervals unless otherwise stated.

	Models without covariates						
	Model 0	Model 1	Model 2	Model 3	Model 4	Model 5	Model 6
Time	0.30 (0.27,0.37)	0.30 (0.26,0.36)	0.30 (0.26,0.36)	0.30 (0.26,0.36)	0.31 (0.27,0.36)	0.31 (0.27,0.36)	0.29 (0.24,0.36)
Age							0.15 (0.05,0.29)
Health authority		0.04 (0.02,0.06)		0.03 (0.01,0.06)			
Ward (spatial)			0.07 (0.04,0.12)	0.07 (0.03,0.12)		0.07 (0.04,0.12)	
Ward (random)					0.07 (0.04,0.11)	0.06 (0.03,0.09)	
Model fit and complexity							
Deviance:							
mean	9008	9000	8971	8972	8976	8954	8514
median	9008	8999	8972	8973	8979	8954	8514
(10%,90%)	(8997,9019)	(8988,9012)	(8950,8994)	(8950,8993)	(8949,9002)	(8932,8977)	(8496,8534)
p_D	12	14	32	33	39	48	19
DIC	9020	9014	9003	9005	9015	9002	8533

	Models with covariates					
	Model 7	Model 8	Model 9	Model 10	Model 11	Model 12
Time	0.29 (0.24,0.36)	0.30 (0.25,0.36)	0.29 (0.25,0.37)	0.30 (0.25,0.38)	0.30 (0.25,0.37)	0.18(0.13,0.27) 0.18(0.09,0.28) 0.32(0.21,0.50)
Age	0.13 (0.04,0.29)	0.13 (0.04,0.28)	0.14 (0.05,0.30)	0.14 (0.05,0.30)	0.13 (0.05,0.27)	0.12 (0.04,0.26)
Health authority	0.04 (0.02,0.07)		0.04 (0.01–0.07)			
Ward (spatial)		0.14 (0.08,0.18)	0.14 (0.09,0.18)		0.11 (0.05,0.17)	0.11 (0.06,0.16)
Ward (random)				0.14 (0.09,0.18)	0.10 (0.04,0.15)	
Model fit and complexity						
Deviance:						
mean	8503	8430	8431	8414	8403	8409
median	8502	8431	8431	8414	8402	8409
(10%,90%)	(8485,8530)	(8396,8464)	(8401,8462)	(8377,8451)	(8367,8440)	(8377,8438)
p_D	22	69	69	94	91	60
DIC	8525	8499	8500	8508	8494	8469

similar across all models. It was fairly constant for 45 to 75 years (90 per cent of patients), with an indication of a lower risk for younger ages and decreasing for older ages (but sparse data as indicated by frequency points on the figure). There were no differences in time to

Table III. Effect of health authority area, ward area, sex and disease severity on time to CABG. Values are posterior approximated *hazard ratio* (*HR*) estimates with 95 per cent credible intervals comparing female versus male and two and three diseased vessels (2DV and 3DV) versus 1 DV and each health authority and ward compared to the overall mean. The range of median estimates are given for ward effects.

	Model 1	Model 2	Model 3	Model 4	Model 5	Model 6
Health authority						
ELCHA	0.96 (0.90,1.03)		1.00 (0.91,1.11)			
B&H	1.04 (0.97,1.14)		1.02 (0.94,1.13)			
R&WF	0.92 (0.86,0.99)		0.96 (0.88,1.05)			
S ESS	1.02 (0.96,1.13)		0.99 (0.89,1.10)			
N ESS	1.04 (0.96,1.12)		1.02 (0.92,1.13)			
Ward (spatial)		(0.84–1.15)	(0.87–1.12)		(0.85,1.13)	
Ward (random)				(0.90,1.09)	(0.94,1.07)	
Female						0.97 (0.88,1.06)
Disease						
2DV						2.11 (1.90,2.35)
3DV						2.67 (2.43,2.93)

	Model 7	Model 8	Model 9	Model 10	Model 11	Model 12
Health authority						
	0.98 (0.91,1.05)		0.99 (0.88,1.13)			
	1.07 (0.98,1.17)		1.04 (0.93,1.17)			
	0.91 (0.84,0.98)		0.98 (0.88,1.09)			
	1.00 (0.94,1.08)		0.97 (0.85,1.10)			
	1.07 (1.01,1.13)		1.01 (0.90,1.12)			
		(0.68,1.39)	(0.68,1.36)		(0.75,1.28)	(0.74–1.27)
				(0.75, 1.47)	(0.86,1.19)	
	0.96 (0.87,1.06)	0.96 (0.87,1.07)	0.96 (0.87,1.07)	0.96 (0.87,1.07)	0.96 (0.87,1.06)	0.96 (0.88,1.06)
Disease						
	2.11 (1.93,2.36)	2.14 (1.93,2.38)	2.15 (1.93,2.40)	2.18 (1.95,2.43)	2.18 (1.95,2.45)	
	2.68 (2.41,2.95)	2.73 (2.45,3.03)	2.73 (2.47,3.03)	2.76 (2.48,3.06)	2.77 (2.51,3.09)	

*Health authority: ELCHA = East London and City; B&H = Barking and Havering; R&WF = Rebridge and Waltham Forrest; S ESS = South Essex; N ESS = North Essex.

CABG between men and women with the HR = 0.97 (0.88,1.06). Number of diseased vessels had a significant impact on time to CABG with HR of 2.11 for two-vessel disease and 2.67 for three-vessel disease, compared to one-vessel disease.

Fitting the spatial ward effect adjusting for these covariates (model 8) increased the marginal SD for the spatial effect to 0.14 (0.08,0.18) (compared to 0.07 from model 2). The effect size range increased from minimum of 0.68 to 1.39 maximum, DIC = 8499 (change from model 6 = 34).

Figure 4 shows the spatial effect of time to CABG after adjusting for individual covariates. Areas with increased risk of CABG were found in Chelmsford and Malden in North Essex, while areas less likely to perform CABG procedures were found in and around Harlow in North Essex and Walthamstow and Chingford in North East London (Redbridge and Waltham Forrest HA). The second map in Figure 4 shows the corresponding posterior probabilities of the area effects categorized as for Figure 2. Note that the spatial pattern was more pronounced

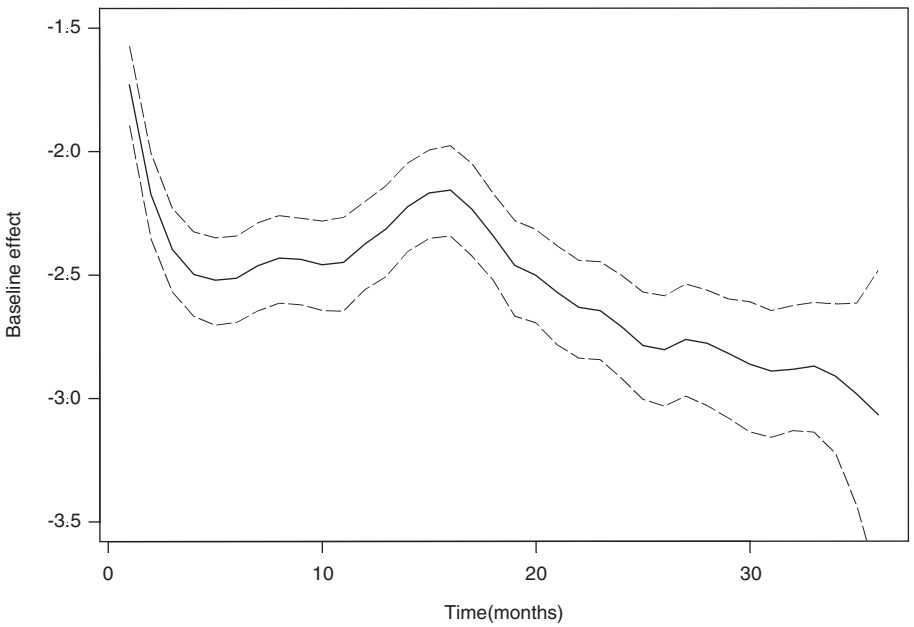

Figure 1. Baseline effect for model 0:Baseline, on a probit scale, posterior median estimates (solid) and 95 per cent credible intervals (dashed).

than for model 1 without covariates. Again when HA was included (model 9) this had very little effect on the estimates and DIC.

Unstructured random effects (models 10 and 11)

Unstructured effects typically have a better fit than structured effects as they have less dependence *a priori* and so are more complex as reflected by the higher $p_D = 94$ for model 10 compared to 69 from model 8 with the spatial effect. Overall this model is 'as good as' model 8 in terms of DIC.

Model 11 (like model 5) separates the area effect into two parts: structured and unstructured random effects. While both attempt to capture unobserved factors, some of these may be more spatially correlated than others. Here the marginal SD for the spatial part reduced to 0.11 (compared to 0.14 in model 5) and the unstructured reduced slightly more to 0.10 compared to 0.14 in model 9. We can conclude that the unmeasured spatial covariates are of slightly more importance than the unstructured random effects. Summing the estimates for the structured and unstructured random effects (using the stored samples) gave a range of HRs of 0.67–1.39, very similar to what was found in the spatial model. Like model 10, in terms of model fit and complexity, this model was also comparable to model 8.

All previous models assume that the discrete baseline hazards for one-, two- and three-vessel disease are parallel and have the same form. Figure 5 shows the separate baseline effects from model 8 assuming a fixed disease severity effect corresponding to hazard ratios of 2.14 and 2.73 for two- and three-vessel disease, respectively, compared to one-vessel disease.

Figure 2. Spatial effect from model 2:Baseline+Ward(spatial). Top map shows hazard ratios (HR) per area compared to the overall mean. Lower map shows respective posterior probabilities of $HR > 1$: < 5 per cent white, 5–95 per cent grey, > 95 per cent black.

Model incorporating separate baseline effects for number of diseased vessels (model 12)

As a check of the proportional hazards assumption, we estimated a separate baseline hazard for each level of disease severity (the most important covariate) by including time varying covariate effects. Model 12 allows for different baselines for each level of disease severity, that is

$$P(T = t \mid T \geqslant t) = \Phi(f_0(t) + f_1(\text{age}) + f_2(\text{ward}) + \text{DV2}^* f_3(t) + \text{DV3}^* f_4(t) + x'\beta)$$

The separate baselines $f_0(t)$, $f_0(t) + \text{DV2}^* f_3(t)$ and $f_0(t) + \text{DV3}^* f_4(t)$ for 1DV, 2DV and 3DV, respectively, are shown in Figure 6. It can be seen that for single vessel disease, unlike for two- and three-vessel disease, the baseline remained fairly constant after an initial decrease in the first few months. Between months 10 and 20 the difference in baseline hazards for one-, two- and three-vessel disease were at their greatest.

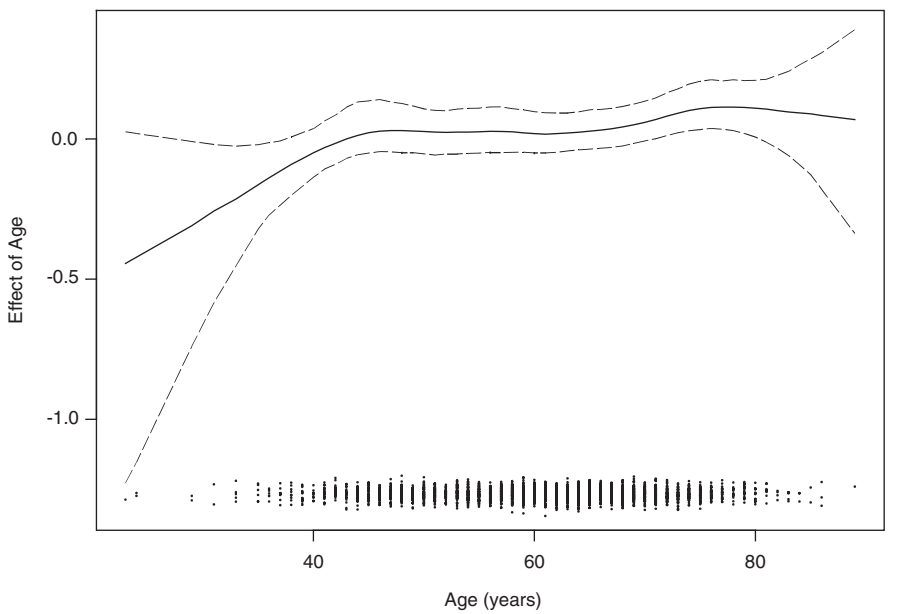

Figure 3. Effect of age from model 8:Baseline+Age+Female+Num2+Num3+Ward(spatial), on a probit scale, posterior median estimates (solid) and 95 per cent credible intervals (dashed). Frequency of observations at each year of age is indicated by the dots.

The superiority of this model was indicated by a further reduction in the posterior mean deviance and DIC = 8469. The spatial pattern (Figure 7) was slightly reduced to a range of HRs 0.74–1.27 and marginal SD of 0.11.

We also fitted models including interactions between age and the baseline and age and number of diseased vessels (details not shown). Neither of these models improved in terms of DIC and the spatial effect remained unchanged.

Sensitivity to hyperparameter choice

Results from using different hyperparameter values are given in Table IV for selected models. We found that changing these values had little impact on the majority of the effects, apart from age. Here the marginal SD notably decreased with decreasing value of b, producing a smoother effect overall.

To test the reliability of the p_D and DIC estimates we ran models 7,8 and 10 for over 200000 iterations and found that the results did not change (details not shown).

DISCUSSION

We set out to measure and describe the spatial variation in time to CABG before and after adjustment for individual specific covariates. We believe this paper demonstrates the applicability of using a Bayesian spatial survival model to examine small area variations in operation

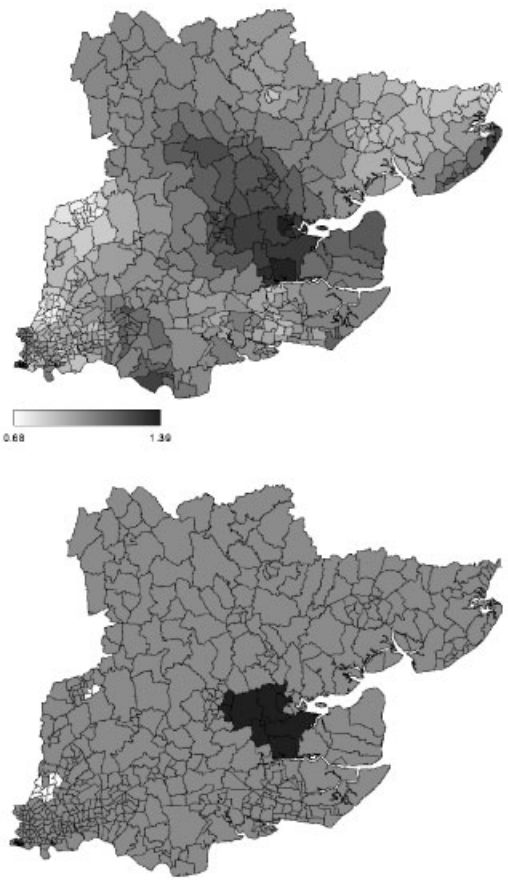

Figure 4. Spatial effect on time to CABG from model 8:Baseline+Age+Female+2DV+3DV+Ward(spatial). Top map shows hazard ratios (HR) per area compared to the overall mean. Darker areas indicating increased risk of CABG. Lower map shows respective posterior probabilities of $HR > 1$: < 5 per cent white, 5–95 per cent grey, > 95 per cent black.

waiting times, adjusting for key individual level covariates. Ward level spatial effect sizes for the 'disease maps' were estimated from Bayesian hierarchical models. Estimates from the model including the number of diseased vessels and other covariates (model 8) gave a range of hazard ratios from 0.68 to 1.39. This two-fold difference between wards with the lowest and highest risk of CABG, among patients who had all undergone angiography at a single centre, warrants further investigation. When time varying covariates were included in the model (model 12), we found some evidence of non-proportional hazards, with single vessel disease displaying a more constant baseline effect over time compared to two- and three-vessel disease. The spatial effect for this model reduced to a 1.7-fold difference, HRs ranging from 0.74 to 1.27.

We found evidence of a marked spatial effect on time to CABG only in the presence of individual covariates. Models without covariates showed less evidence of a spatial effect. This

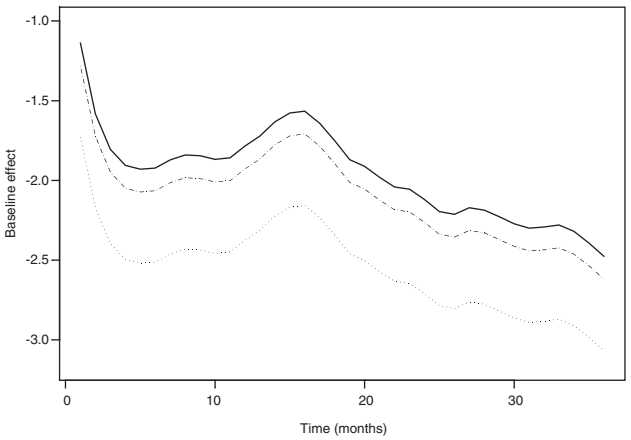

Figure 5. Baseline effects for model 8:Baseline+Age+Female+2DV+3DV+Ward(spatial) on a probit scale, posterior median estimates for one-vessel (small dots), two-vessel (large dots), and three-vessel (solid line) disease.

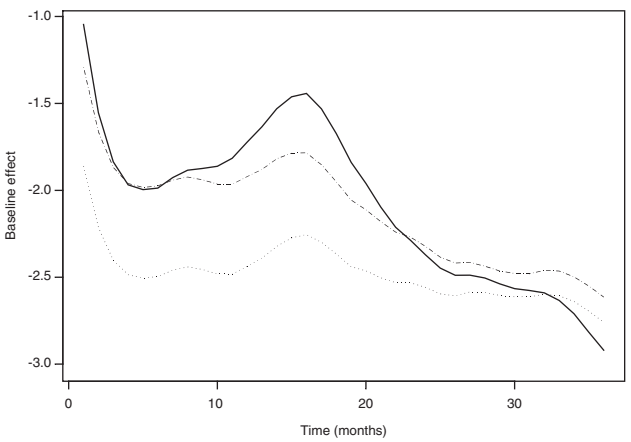

Figure 6. Baseline effects for model 12:Baseline+2DV*Baseline +3DV*Baseline+Age+Female+Ward(spatial) on a probit scale, posterior median estimates for one-vessel (small dots), two-vessel (large dots), and three-vessel (solid line) disease.

observed increase in spatial variation for the model with covariates (model 8) compared to the model without covariates (model 2) is contrary to that often observed in disease mapping studies. Usually the inclusion of aggregated covariates contributes to a decrease in the spatial variation as it is being 'explained away'. This emphasizes the necessity of having individually measured covariates – a particular strength of the ACRE study. The analysis presented here is not currently possible using routine sources of data because the number of diseased vessels is not collected.

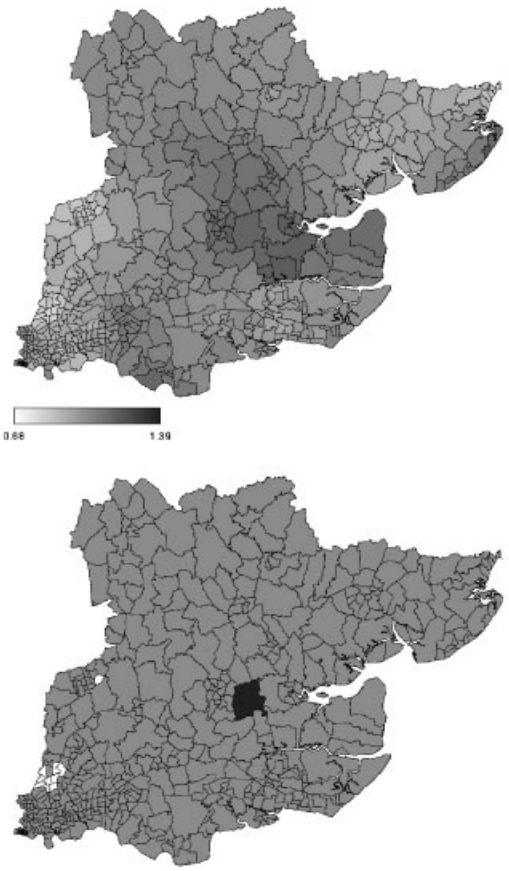

Figure 7. Spatial effect on time to CABG from model 12:Baseline+2DV*Baseline+3DV*Baseline Age+Female+Ward(spatial). Top map shows hazard ratios (HR) per area compared to the overall mean. Darker areas indicating increased risk of CABG. Lower map shows respective posterior probabilities of HR > 1: < 5 per cent white, 5–95 per cent grey, > 95 per cent black.

Adopting a spatial disease mapping approach to measure the geographical variation provides a clear visual representation of how location of residence affects waiting time to CABG. An Austrian study adopted an alternative spatial disease mapping method, using Moran's *I* statistic, to examine the spatial area risk of PTCA [27], but not for procedure waiting time. The advantage of the spatial analysis lies in the ability to identify smaller areas of increased and decreased risk. Comparing the results with a standard Cox proportional hazards (PH) model, fitting health authority using dummy variables indicated that patients in North East London (Redbridge and Waltham Forrest) and in East London were less likely than patients in North Essex to undergo CABG. While this is consistent with our results on the smaller ward level, it does not exploit the potential spatial aspect of the data on the smaller area scale. We identified areas of both increased (Chelmsford) and decreased (Harlow) risk within North Essex health authority, which is lost in the Cox PH model. Comparing our Bayesian models with and without including health authority (model 9 versus model 8) showed no

Table IV. Sensitivity to choice of hyperparameter values for selected models. Values are marginal SDs and 95 per cent credible intervals.

		$a=1,\ b=0.00005$ for rw2, else $a=1,\ b=0.005$ (reported results)	$a=1,\ b=0.00005$ for all effects	$a=1,\ b=0.005$ for all (BayesX default)	$a=0.00005,\ b=0.00005$ for all effects	$a=1,\ b=0.05$ for all effects
Model 8	Baseline	0.30 (0.25,0.36)	0.29 (0.25,0.37)	0.30 (0.25,0.37)	0.30 (0.25,0.38)	0.31 (0.26,0.41)
	Age	0.13 (0.04,0.28)	0.13 (0.05,0.28)	0.24 (0.10,0.52)	0.16 (0.06,0.35)	0.34 (0.13,0.99)
	Ward (spatial)	0.14 (0.08,0.18)	0.13 (0.07,0.18)	0.13 (0.09,0.18)	0.14 (0.09,0.19)	0.15 (0.11,0.19)
Model fit	$\bar{D}$	8431	8434	8424	8426	8406
	p_D	69	66	74	71	88
	DIC	8499	8500	8498	8497	8494
Model 10	Baseline	0.30 (0.25,0.38)	0.29 (0.24,0.37)	0.30 (0.25,0.36)	0.32 (0.12,0.84)	0.31 (0.25,0.41)
	Age	0.14 (0.05,0.30)	0.15 (0.05,0.29)	0.29 (0.11,0.60)	0.16 (0.06,0.34)	0.39 (0.14,0.96)
	Ward (random)	0.14 (0.09,0.18)	0.14 (0.09,0.18)	0.14 (0.10,0.19)	0.14 (0.10,0.19)	0.16 (0.12,0.20)
Model fit	$\bar{D}$	8414	8414	8403	8408	8383
	p_D	94	94	83	97	102
	DIC	8508	8508	8486	8505	8485
Model 7	Baseline	0.29 (0.24,0.36)	0.29 (0.25,0.37)	0.29 (0.24,0.37)	0.30 (0.25,0.38)	0.30 (0.25,0.39)
	Age	0.13 (0.04,0.29)	0.14 (0.05,0.28)	0.25(0.1,0.52)	0.16 (0.05,0.33)	0.32 (0.12,0.84)
	Health authority	0.04 (0.02,0.07)	0.01 (0.00,0.03)	0.04 (0.02,0.07)	0.02 (0.00,0.05)	0.05 (0.03,0.08)
Model fit	$\bar{D}$	8503	8511	8496	8504	8486
	p_D	22	20	27	23	34
	DIC	8525	8531	8523	8527	8520

improvement in terms of DIC, indicating the relative importance of ward area over health authority area effect on time to CABG.

We modelled the baseline hazard and age non-parametrically using smoothing priors. While a non-parametric estimation of the baseline is often used in extended proportional hazard models, it is not as common to model age in this way. Use of smoothing priors has the advantage that age (or any other continuous covariate) can be incorporated in the model without categorization using arbitrary cut-offs, or having to assume a specific parametric form (for example, linear or quadratic). We observed that the baseline hazard was initially high which is consistent with emergency CABG directly after angiography. The increase in risk between 6 and 16 months reflects the typical waiting time experience for CABG patients in England. We found the effect of age on time to CABG was fairly constant for 45 to 75 years, with an indication of a lower risk for younger ages.

A potential disadvantage of the Markov random field approach for the spatial smoothing is that it assumes *a priori* that the degree of smoothness is constant over the whole study area. This issue also applies to the smoothing model for the baseline hazard and age effects. More adaptive (spatial) smoothing methods have recently been proposed [28, 29] for disease mapping. However, while the applicability of such models to data adjusting for one covariate has been explored [30], further work is still needed for adjusting for more than one covariate. An extension that we considered was the inclusion of individual specific random effects, that is, frailties, in the model. Similar discrete time survival models with frailties and non-parametric temporal effects have recently been described [31]. However, for our application this complexity failed and the MCMC algorithm did not converge, possibly due to non-identifiability between covariate effects and frailties, that is, the effect of unobserved covariates.

The observed small area spatial variation in time to CABG warrants investigation of three inter-related sets of explanatory factors. First, individual patient clinical covariates, which define the appropriateness [17] and urgency [32] for CABG, may contribute to area differences in the need and demand for CABG. Second, factors associated with the supply of the health care system including distance to the tertiary centre [33–35] and the nature of the referral and decision making process may also contribute to the observed spatial pattern. For example, if cardiologists have a preference for angioplasty this may contribute to the localized areas of lower CABG risk. Third, characteristics of the areas in which the patients live may have an impact, as previous studies have reported area social deprivation is associated with rate of revascularization [14, 36]. All of these explanatory factors are to be investigated in this data set.

APPENDIX: BAYESX CODE

The following gives the BayesX commands that were used to run selected models:

Model 2

```
b.regress CABGD=TIME(rw2, a=1.0, b=0.00005)+WARD(spatial,map=ACRE),
iterations=11000 burnin=1000 step=10 family=binomialprobit predict using
cabgdata
```

Model 7

```
b.regress CABGD=TIME(rw2, a=1.0, b=0.00005)+AGE
```



```
(rw2, a=1.0, b=0.00005)
+SEX+NUM2+NUM3+HA(random), iterations=11000 burnin=1000 step=10
family=binomialprobit predict using cabgdata
```

Model 8

```
b.regress CABGD=TIME(rw2, a=1.0, b=0.00005)+AGE
(rw2, a=1.0, b=0.00005)
+SEX+NUM2+NUM3+WARD(spatial,map=ACRE), iterations=11000 burnin=1000
step=10 family=binomialprobit predict using cabgdata
```

Model 10

```
b.regress CABGD=TIME(rw2, a=1.0, b=0.00005)+AGE
(rw2, a=1.0, b=0.00005)
+SEX+NUM2+NUM3+WARD(random), iterations=11000 burnin=1000 step=10
family=binomialprobit predict using cabgdata
```

Model 12

```
b.regress
CABGD=TIME(rw2, a=1.0, b=0.00005)+NUM2*TIME(rw2, a=1.0, b=0.00005)+NUM3*TIME
(rw2, a=1.0, b=0.00005)+AGE(rw2, a=1.0, b=0.00005)+SEX+WARD(spatial,
map=acre, a=1.0, b=0.005), interactions=11000 burnin=1000 step=10
family=binomialprobit predict using cabgdata
```

ACKNOWLEDGEMENTS

We would like to thank Kees de Hoogh for extracting the boundary data and ward adjacencies for drawing maps and estimating the spatial effects; Stefan Lang for help with BayesX; Sylvia Richardson for her helpful comments on earlier drafts and the two referees for their constructive comments. AMC is supported by a Medical Research Council Collaborative Research Studentship (G78/6708). HH is supported by a Public Health Career Scientist Award from the Department of Health.

REFERENCES

1. Diez-Roux AV, Nieto FJ, Muntaner C, Tyroler HA, Comstock GW, Shahar E, Cooper LS, Watson RL and Szklo M. Neighbourhood environments and coronary heart disease: a multilevel analysis. *American Journal of Epidemiology* 1997; **146**:48–63.
2. Sundquist J, Malmstrom M, Johansson SE. Cardiovascular risk factors and the neighbourhood environment: a multilevel analysis. *International Journal of Epidemiology* 1999; **28**:841–845.
3. Besag J, York JC, Mollie A. Bayesian image reconstruction, with two applications in spatial statistics (with discussion). *Annals of Institute of Statistical Mathematics* 1991; **43**:1–59.
4. Fahrmeir L, Lang S. Bayesian inference for generalised additive mixed models based on Markov random field priors. *Journal of the Royal Statistical Society, Series C* (*Applied Statistics*) 2001; **50**:201–220.
5. Banerjee S, Wall MM, Carlin BP. Frailty modeling for spatially correlated survival data, with application to infant mortality in Minnesota. *Biostatistics* 2002; **40**:123–142.
6. Osnes K, Aalen OO. Spatial smoothing of cancer survival: a Bayesian approach. *Statistics in Medicine* 1999; **18**:2087–2099.
7. Efron B. Logistic regression, survival analysis and the Kaplan-Meier Curve. *Journal of the American Statistical Association* 1988; **83**:414–425.
8. Fahrmeir L. Dynamic modelling and penalised likelihood estimation for discrete time survival data. *Biometrika* 1994; **81**:317–330.
9. Fahrmeir L. Discrete survival-time models. In *Encyclopedia of Biostatistics*, Armitage P (ed.). Wiley: Chichester, 1998; 1163–1168.
10. Fahrmeir L, Tutz G. *Multivariate Statistical Modelling Based on Generalised Linear Models.* Springer: New York, 2001.

11. Department of Health. Saving Lives: Our Healthier Nation. 1999.
12. Carroll RJ, Horn SD, Soderfeldt B, James BC, Malmberg L. International comparison of waiting times for selected cardiovascular procedures. *Journal of the American College of Cardiology* 1995; **25**:557–563.
13. Rosanio S, Tocchi M, Cutler D, Uretsky BF, Stouffer GA, deFilippi CR, MacInerney EJ, Runge SR, Aaron J, Otero J, Garg S and Runge MS. Queuing for coronary angiography during severe supply-demand mismatch in a US public hospital: analysis of a waiting list registry. *Journal of the American Medical Association* 1999; **282**:145–152.
14. Alter DA, Naylor CD, Austin P, Tu JV. Effects of socioeconomic status on access to invasive cardiac procedures and on mortality after acute myocardial infarction. *New England Journal of Medicine* 1999; **341**:1359–1367.
15. Ben Shlomo Y, Chaturvedi N. Assessing equity in access to health care provision in the UK: does where you live affect your chances of getting a coronary artery bypass graft? *Journal of Epidemiology and Community Health* 1995; **49**:200–204.
16. Black N, Langham S, Petticrew M. Coronary revascularisation: why do rates vary geographically in the UK? *Journal of Epidemiology and Community Health* 1995; **49**:408–412.
17. Hemingway H, Crook AM, Feder G, Banerjee S, Dawson JR, Magee P, Philpott S, Sanders J, Wood A and Timmis AD. Underuse of coronary revascularization procedures in patients considered appropriate candidates for revascularization. *New England Journal of Medicine* 2001; **344**:645–654.
18. Spiegelhalter D, Best NG, Carlin BP, Van der Linde A. Bayesian measures of model complexity and fit. *Journal of the Royal Statistical Society, Series B* 2002 (in press).
19. Lang S, Brezger A. BayesX: software for Bayesian inference based on Markov chain Monte Carlo simulation techniques. (0.9). University of Munich, 2002. Available at http://www.stat.uni-muenchen.de/~lang/bayesx/bayesx.html.
20. Spiegelhalter D, Thomas A, Best NG. WinBUGS version 1.3 user manual. MRC Biostatistics Unit, Cambridge. Available at http://www.mrc-bsu.cam.ac.uk/bugs 2000.
21. Fahrmeir L, Knorr-Held L. Dynamic and semiparametric models. In *Smoothing and Regression*: *Approaches*, *Computation and Application*, Michael Schimek (ed.). Wiley: New York, 2000; 513–544.
22. Thompson WA, Jr. On the treatment of grouped observations in life studies. *Biometrics* 1977; **33**:463–470.
23. Rue H. Fast sampling of Gaussian Markov random fields. *Journal of the Royal Statistical Society, Series B* 2001; **63**:325–338.
24. Fahrmeir L, Lang S. Bayesian semiparametric regression analysis of multicategorical time-space data. *Annals of the Institute of Statistical Mathematics* 2001; **52**:1–18.
25. Carroll RJ, Ruppert D, Stefanski LA. *Measurement Error in Nonlinear Models.* Chapman and Hall: 1995.
26. Holmes CC, Knorr-Held L. Efficient simulation in Bayesian logistic regression models. *Technical Report, Imperial College London, Department of Mathematics* 2003.
27. Strauss R, Pfeifer C, Ulmer H, Muhlberger V, Pfeiffer KP. Spatial analysis of Percutaneous Transluminal Coronary Angioplasty (PTCA) in Austria. *European Journal of Epidemiology* 1999; **15**:451–459.
28. Knorr-Held L, Rasser G. Bayesian detection of clusters and discontinuities in disease maps. *Biometrics* 2000; **56**:13–21.
29. Denison DG, Holmes CC. Bayesian partitioning for estimating disease risk. *Biometrics* 2001; **57**:143–149.
30. Giudici P, Knorr-Held L, Rasser G. Modelling categorical covariates in Bayesian disease mapping by partition structures. *Statistics in Medicine* 2000; **19**:2579–2593.
31. Biller C. Discrete duration models combining dynamic and random effects. *Lifetime Data Analysis* 2000; **6**: 375–390.
32. Naylor CD, Sykora K, Jaglal SB, Jefferson S. Waiting for coronary artery bypass surgery: population-based study of 8517 consecutive patients in Ontario, Canada. *Lancet* 1995; **346**:1605–1609.
33. Gaffney B, Kee F. Predictors for waiting time for coronary angioplasty in a high risk population. *Quality in Health Care* 1995; **4**:244–249.
34. Gregory PM, Malka ES, Kostis JB, Wilson AC, Arora JK, Rhoads GG. Impact of geographic proximity to cardiac revascularization services on service utilization. *Medical Care* 2000; **38**:45–57.
35. Hippisley-Cox J, Pringle M. Inequalities in access to coronary angiography and revascularisation: the association of deprivation and location of primary care services. *British Journal of General Practice* 2000; **50**:449–454.
36. Pell JP, Pell AC, Norrie J, Ford I, Cobbe SM. Effect of socioeconomic deprivation on waiting time for cardiac surgery:retrospective cohort study. *British Medical Journal* 2000; **320**:15–18.

